

# EEG Detection of Early Alzheimer's Disease Using Psychophysical Tasks

Robert Sneddon, William Rodman Shankle, Junko Hara,  
Anthony Rodriguez, Donald Hoffman and Utpal Saha

## Key Words

Alzheimer's Disease, Early Detection  
Alzheimer's Disease, Related Disorders  
Cognitive Impairment, Mild  
Electroencephalography  
Quantitative EEG

## ABSTRACT

In this study, we hypothesized that a quantitative EEG (qEEG) method for measuring EEG variability combined with specific psychophysical tasks could improve the classification accuracy of subjects with normal aging vs. mild cognitive impairment (MCI) or mild dementia due to Alzheimer's Disease and Related Disorders (ADRD). The cross-sectional sample consisted of 48 subjects (32 normal aging and 16 ADRD:  $n=3$  mild dementia,  $n=13$  MCI FAST stage 3).

During EEG recording, subjects performed two visual, delayed recognition memory tasks as well as a task that tested their ability to perceive structure-from-motion (SFM). These EEG data were used to compute qEEG measures of the (normalized) variance of posterior cortical activity during the first 150 milliseconds (ms) after stimulus onset and the variance of anterior cortical activity during the second 150 ms epoch. The ratio, anterior/posterior cerebral qEEG value, was then computed for each subject, and the optimal cutoff value identified to discriminate normal from impaired subjects.

An optimal qEEG cutoff value for the delayed recognition memory tasks correctly discriminated 30 of the 32 normal aging subjects (94% specificity) and 14 of 16 MCI-to-mild ADRD subjects (88% sensitivity). On the other hand, the application of this qEEG measure to EEG data recorded while subjects performed a SFM task did not distinguish between ADRD and normal aging any better than chance.

In conclusion, this qEEG measure is specific to the psychophysical task being performed by the subject. When it was combined with delayed recognition memory tasks, it yielded results that are comparable to the accuracies reported by PET scan studies of normal aging vs. AD with mild cognitive impairment. These results warrant further evaluation.

## INTRODUCTION

The EEG is a scalp recording of the brain's electrical activity. This electrical activity may reflect the task that the brain is performing at the time of the EEG recording. For example, if a person is looking at a face and trying to remember if they have seen it before, their EEG recording might reflect this fact. Likewise, if a person is engaged in a different task, such as watching the motion of dots moving in the manner of a rigid object, "structure from motion" (SFM), their EEG might reflect that task. If this is true, then the structure from motion EEG would be different from the EEG recorded while a person is trying to remember a face.

In this study we will take this hypothesis and quantify it for the purpose of detecting very mild to mild Alzheimer's Disease and Related Disorders (ADRD). We will do this by examining the EEG data of subjects, normal aging or having very mild to mild ADRD, who are performing psychophysical tasks. Some of these tasks ought to be relevant to the detection of ADRD. Those tasks are delayed recognition memory tasks. Another task might not be relevant to the detection of ADRD. That task is perceiving structure from motion. We hypothesize that a relevant quantitative EEG (qEEG) method will distinguish between normal aging and ADRD subjects who are engaged in delayed recognition memory tasks, but not between normal aging and ADRD subjects who are engaged in perceiving structure from motion. The qEEG measure that we used is a measure of the short-term changes in the EEG waveform or "rapid variance." This measure, which relates to the synchrony of local neuronal activity, may correspond to the information in the EEG waveform.<sup>1-3</sup>

## The Relevance of Delayed Recognition Memory to Early Alzheimer's Disease

In Alzheimer's disease (AD), delayed recognition or episodic memory loss is the earliest clinical change.<sup>4-7</sup> Pathophysiological, electrophysiological, psychophysical and clinical measures of this characteristic are consistent;

Robert Sneddon, PhD, William Rodman Shankle, MS, MD, Junko Hara, PhD, Anthony Rodriguez, PhD, Donald Hoffman, PhD, and Utpal Saha, BS, are from the University of California at Irvine, California.

Address requests for reprints to Robert Sneddon, PhD, 125 S. Holliston Ave., #6, Pasadena, CA 91106, USA. Email: rsneddon@alumni.caltech.edu

Received: October 19, 2004; accepted: April 20, 2005.

in Alzheimer's disease, the first portion of the brain to decline is the hippocampal area including the transentorhinal and entorhinal cortices, the hippocampal formation, and associated parahippocampal cortices.<sup>8</sup> Fluoro-2-deoxy-D-glucose Positron Emission Tomography (FDG PET) studies show a general glucose metabolic deficiency in the temporal and parietal association areas. These deficiencies are in excess of what would be expected by the degree of brain atrophy associated with AD.<sup>9</sup> Further FDG PET studies suggest that the very first area affected by AD is the entorhinal cortex. The appearance of lesions in this area is followed by lesions in the hippocampus and associated parahippocampal cortices.<sup>10</sup> In turn, these areas are strongly implicated in the production of delayed recognition memories.<sup>11-19</sup> For this reason, the EEG of an AD/DRD subject who is engaged in a delayed recognition task is hypothesized to differ from that of a normal aging subject.

### EEG, ERP, and fMRI Studies of Delayed Recognition

Delayed recognition involves both the working memory (attentive recognition; dorsolateral prefrontal cortex, "DLPFC") and episodic memory (delayed retrieval; the hippocampus and parahippocampal cortices).<sup>11-21</sup> There are a number of working memory/delayed recognition EEG, ERP, and fMRI studies both for normal aging individuals and AD/DRD individuals. An fMRI study shows that the most active areas of the P300 working memory task are the supramarginal gyrus, superior parietal lobule (part of posterior parietal cortex), the posterior cingulate gyrus, thalamus, inferior occipitotemporal cortex, insula, DLPFC, anterior cingulate cortex, medial frontal gyrus, premotor area, and cuneus.<sup>22</sup> Other fMRI studies of working memory implicate the DLPFC and the inferior/posterior parietal cortex.<sup>23,24</sup> Event related potential (ERP) studies of the working memory of normal aging individuals show significant evoked potentials for striate/extrastriate cortex at about 130 ms.<sup>25,26</sup> Posterior parietal cortex shows significant activity, "electrogenesis," at 40 ms and again at 100 ms (in somatosensory working memory tasks).<sup>24,27</sup> It is important to note that these latter studies did not use standard EEG averaging to deduce the ERP. Instead they used a non-averaging statistical technique, the "Z method." Further in time, the N170 and the vertex-positive potential (VPP) occur and are often associated with face recognition tasks (fusiform gyrus for the N170; ventral stream activity); however, this effect is sometimes also seen in object and word recognition.<sup>28</sup>

There are a number of working memory/delayed recognition studies on the activation of prefrontal cortex. The earliest ERP time seen is 140 ms.<sup>24</sup> This ERP is centered in the DLPFC. Again, this study uses the "Z method," which means that this time is not necessarily at the peak of the activity. There is actually a large range for this time, 100-180 ms. Other studies show later times; for example, 150 ms and 190 ms, followed by "triphasic" activity at 200-285-350 ms.<sup>29</sup> Guillaume and Tiberghien<sup>30</sup>

found a prefrontal ERP peak at 200 ms. Similarly, another study shows prefrontal activity peaking at 250 ms and then moving towards centro-parietal cortex at 350 ms and arriving at parietal-occipital cortex at 450 ms.<sup>31</sup> ERP studies of word recognition impairment in schizophrenics suggest that this impairment begins about 200-300 ms (N2-P3) after stimulus onset.<sup>32</sup> Johnson and Olshausen<sup>25</sup> conclude that recognition occurs 150-300 ms after the stimulus onset. Furthermore, the delayed recognition type of memory retrieval is monitored, and possibly initiated, by the DLPFC (and apparently also monitored by frontopolar/anterior prefrontal cortex).<sup>33-35</sup>

The EEG spectral hallmark in AD is decreased alpha and beta power and increased theta power.<sup>36</sup> The later stages of AD also show increasing delta power. The increased absolute and relative theta power correlates well with cognitive dysfunction.<sup>37</sup> This EEG activity also provides good discrimination between different levels of AD severity.<sup>38</sup> Moreover, AD patients show a background EEG slowing with reduced fast activity and coherence.<sup>39,40</sup> The working memory old/new effect (P300) is faster and stronger in younger individuals than in older individuals, who, in turn, tend to have faster and stronger P300 effects than AD/DRD individuals.<sup>41,43</sup> Working memory EEG of AD subjects tends to have less synchronization in the upper alpha (10-12 Hz) and beta bands than MCI subjects. On the other hand, MCI subjects tended to have greater lower alpha (8-10 Hz) synchronization than normal aging subjects.<sup>44</sup> Similarly, Hogan et al<sup>45</sup> found decreased upper alpha coherence for MCI AD subjects between central and right temporal cortex. On the other hand, Rugg et al<sup>46</sup> found no difference between MCI AD and normal aging ERPs for a working memory task.

### EEG Monitoring Congruent with Delayed Recognition Neurophysiology

We sought to monitor subjects' EEGs in a manner congruent with the neurophysiology of delayed recognition. The studies described above show that initial dorsal stream activity is strongest for the posterior parietal cortex and is followed by activation of the DLPFC. Therefore, the goal of the present study was to use time intervals that cover the majority of the activity at the posterior parietal cortex and at the DLPFC. The time interval we used for the posterior parietal cortex is 0-150 ms. Since studies show activity at 40 ms and 100 ms, we can safely conclude that this time interval covers the majority of the initial dorsal stream posterior parietal activity.

Prefrontal activity is more complex. The earliest ERP time shown is 140 ms. However, because of the methods used, this time may mark the start of activity, not the peak of activity. All other studies show later times: 150 ms, 190 ms, 200 ms, 250 ms, and 285 ms. This activity appears to be moving back toward posterior cortex by about 350 ms. Thus, our study made the judicious choice of a time inter-

val of 151-300 ms for prefrontal activity, in agreement with the conclusion of Johnson and Olshausen.<sup>25</sup> This time interval may miss some initial activity and some final activity but it appears to capture the majority of the DLPFC activity which was a goal of this study.

### **The Non-relevance of SFM to Early Alzheimer's Disease**

The perception of SFM is a process attributed to the mid-temporal (MT) area of the cortex.<sup>47-49</sup> It is not a process associated with the hippocampus or parahippocampal cortices, the cortices which are affected by early AD. For this reason, we hypothesize that the EEG of an early AD subject engaged in perceiving SFM will not differ significantly from normal aging subjects.

The present paper tests this hypothesis by the development and application of a quantitative EEG (qEEG) method that is specific to the psychophysical task that the subject is performing. We hypothesize that qEEG measures of similar tasks will produce similar values. qEEG measures of dissimilar tasks will produce dissimilar values. Moreover, since the measure is task specific, we hypothesize that it will distinguish between normal aging and AD subjects when subjects are performing a delayed recognition memory task.

## **MATERIALS AND METHODS**

### **Psychophysical Tasks Combined With EEG**

To test subjects' delayed recognition memories, they performed, two separate delayed recognition tasks — one for emotionally neutral, unfamiliar faces and one for common objects, e.g., a spoon. The displays were 12 by 16 cm; faces were both male and female. To encode these faces and objects in their delayed recognition memory, a subject first performed a working memory task. During the working memory task, the subject saw the visual target stimulus for 500 ms on the computer display of a Dell Inspiron 7500 and then saw a second visual stimulus 4 seconds later. The subject pressed a key to indicate (yes/no) whether the two stimuli matched. The subject was tested on 10 pairs of visual stimuli. This testing happened two times; once for faces and once for objects. A distracter task followed that lasted 10 minutes.

Delayed recognition memory was then tested by presenting 20 visual stimuli - 10 of which were presented during the working memory task. Subjects pressed a key indicating whether a given visual stimulus was presented during the working memory task. This task was performed twice; once for faces and once for objects. During this delayed recognition memory task, their EEG was recorded and the EEG data were automatically marked for when each stimulus began.

Structure-from-motion perception was tested by having subjects view displays of eight dots, 3 millimeters in diameter, which were sometimes moving in a random manner and sometimes moved in the manner of a rigid object. That

rigid object was a cube. This cube would rotate at a speed of 180 degrees/second. The total area covered by the random dot display was 6 cm by 6 cm. Subjects viewed 60 instantiations of this movements; 30 random and 30 rigid. Each stimulus lasted 500 ms. If the subject perceived rigid motion they were instructed to press a yes key, and if they did not perceive rigid motion, they pressed a no key.

### **Subjects**

Informed consent was obtained from all subjects. The experimental protocol was reviewed and approved by the Institute Review Board (IRB) of the University of California, Irvine, IRB # 2003-2888. Thirty-two normal aging subjects (mean age = 58, female = 20, male = 12) and 16 patients with AD (mean age = 73, female = 7, male = 9) agreed to participate in this research.

### **Diagnostic Assessment**

Each subject was evaluated with a 2 hour battery of cognitive testing (including the Consortium to Establish a Registry for Alzheimer's Disease, CERAD, neuropsychology test battery), medical history, structured assessment of activities of daily living, neurological and physical examination, and Clinical Demented Rating (CDR) staging of dementia status. Those who showed evidence of cognitive or functional impairments were further evaluated with routine laboratory dementia diagnostic tests and magnetic resonance imaging (MRI). Patients whose MRI showed no abnormality, including no hippocampal atrophy, underwent an FDG PET scan. Reduced activity in entorhinal, hippocampal or posterior cingulate cortical areas was deemed to be consistent with a diagnosis of MCI AD.

### **Status of the AD Subjects**

Thirteen AD patients had mild cognitive impairment (MCI) (Clinical Dementia Rating Scale,<sup>50</sup> CDR score = 0.5; Functional Assessment Staging,<sup>51,52</sup> FAST = 3). Three AD patients had mild dementia (CDR = 1, FAST = 4). All of the FAST stage 4 patients had been on cholinesterase inhibitor treatment for more than a year. Six of the FAST stage 3 AD patients had been on cholinesterase inhibitor treatment for more than a year, 6 had begun cholinesterase inhibitor treatment within the past year, and 1 patient had not begun cholinesterase inhibitor treatment. CERAD memory tests showed that all normal aging subjects had normal memories (using the accepted -1.5 standard deviation criterion).<sup>53,54</sup> Seven of the AD subjects had abnormal CERAD scores. The other 9 had normal scores, due to high intelligence, early detection, and/or cholinesterase inhibitor treatment.

### **Age, Treatment, and Gender Matched Subgroups**

Age, cholinesterase inhibitor treatment, and possibly gender can be confounds in the qEEG detection of AD.<sup>55-59</sup> Therefore, we created matched sample subgroups for normal aging and for AD. Cholinesterase inhibitor treatment has an efficacy period of about 1 year.<sup>60,61</sup> Therefore, the AD matched sample subgroup consisted of all AD

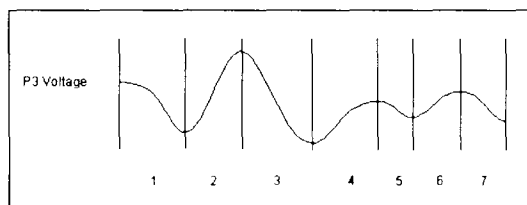


**Figure 1.**  
EEG data separated into rapid variance intervals.

subjects who had not begun cholinesterase inhibitor treatment within the past year. This group consisted of 5 males and 5 females. Similarly, the normal aging subgroup consisted of subjects who were matched for age and gender. This group was composed of the 5 oldest males and the 5 oldest females in the normal aging group. This nearly equated the average age between normal subjects and ADRD subjects; normal aging subjects had an average age of 70, ADRD subjects had an average age of 71. The CDR and FAST ratings of the ADRD subgroup were: 7 subjects at CDR 0.5 (FAST stage 3) and 3 subjects at CDR 1 (FAST stage 4). Seven members of this ADRD matched sample group had abnormal CERAD memory test scores, 3 had normal scores. The total number of subjects in this matched sample analysis was 20.

#### EEG Data Acquisition, Equipment and Electrodes

EEGs were taken using a NeuroScan system. We sampled subjects' EEGs at a rate of 1000 Hz. The DC portion of the EEG was pre-filtered. We also excluded artifacts from the data: eye blinks, muscle movements and 60 Hz interference (caused by electrical coupling with 60 Hz AC sources) during the first 300 ms after the onset of the stimulus. Otherwise, the data were unfiltered. Subjects' data was collected regardless of the correctness or incorrectness of their responses. Subjects needed to complete at least 10 delayed recognition trials in order to compute a reliable qEEG measure whose standard deviation is 2% or less of its value.

#### Electrodes

Subjects were fitted with 28 electrodes on the scalp. The International 10-20 System was used for 21 electrodes.<sup>62</sup> We added an extra 7 electrodes: T7Fp1, T8Fp2, T3C3, T4C4, O1P3, O2P4 and OzPz. T7Fp1 and T8Fp2 were placed on the scalp areas near the left and right DLPFC. T7Fp1 was located in the center of the triangle formed by electrodes Fp1, F3 and F7, and T8Fp2 was located in the center of the electrodes Fp2, F4 and F8 (on the upper edge of each temple).

#### Quantitative Methods

We monitored subjects' EEG in a manner congruent with the neurophysiology of delayed recognition memory. To monitor the early part of a delayed recognition task, we examined the data taken from the electrodes that were

positioned above posterior parietal cortex (area 7) of each brain hemisphere, electrodes P3 and P4. The data recorded by these electrodes were examined for the first 150 ms after the onset of a delayed recognition stimulus. We also examined the data recorded by EEG electrodes located above the DLPFC of each brain hemisphere. The two electrodes used were the non-standard T7Fp1 and T8Fp2. The EEG data examined for these electrodes were those data recorded from 151-300 ms after stimulus onset.

These patterns of cortical activation were measured by examining the changes in EEG variance. This was accomplished by comparing the rapid variance (fast change) of the EEG to the slow variance (slow change) of the EEG. These quantitative methods began with collecting two data sets: DLPFC data and posterior parietal data. These data sets were partitioned into data subsets that correspond to the rapid variance part of the EEG. The data subsets were then used to compute a qEEG measure which compares rapid EEG variance to slow EEG variance. Finally, we compared the anterior to posterior qEEG measures by computing their ratio.

#### Collect DLPFC and Posterior Parietal Data

Two data sets were collected; the posterior parietal cortical data set (0-150 ms, P3 and P4 electrodes) and the DLPFC cortical data set (151-300 ms, T7Fp1 and T8Fp2 electrodes). DLPFC and posterior parietal data interval lengths were slightly altered on each trial so that the DLPFC data set had the exact same number of free variables and total variables as the posterior parietal data set. This makes it possible to directly compare the two data sets.

#### Partition These Data Sets into Rapid Variance Intervals

Each data set was partitioned into rapid variance data intervals that began at a peak, valley or saddle point of an EEG waveform, and ended at the next contiguous peak, valley or saddle point. Quantitatively, this occurs at the places in the time-series EEG data where the discrete derivative is equal to zero. For example, consider an EEG recorded from electrode P3. A 20 millivolt (mv) peak at 8 ms and a -35 mv valley at 20 ms after the visual stimulus onset define one data interval, because it is bounded by critical points, a local maximum and a local minimum. The next rapid variance interval would be defined in the same manner. It would consist of the EEG waveform data from the -30 mv valley to the next voltage peak at 34 ms, 45 mv. See Figure 1 for an example of an EEG waveform partitioned into 7 rapid change intervals; each vertical line represents the start of a new partition. All data were partitioned into rapid variance intervals defined in this manner.

#### Compute the DLPFC and Posterior Parietal qEEG Measures

Each data set, partitioned into rapid variance intervals, was used to compute the following qEEG measure:

Table 1				
ADRD detection: delayed recognition memory				
ADRD FAST Stages 3-4		Normal Aging		Total Accuracy
Sensitivity	Average qEEG Ratio	Specificity	Average qEEG Ratio	Overall
Total Group				
88%	0.92 ± 0.08	94%	1.20 ± 0.06	92%
(14 of 16)	95% CI	(30 of 32)	95% CI	(44 of 48)
Matched Sample Group				
100%	0.85 ± 0.06	100%	1.23 ± 0.08	100%
(10 of 10)	95% CI	(10 of 10)	95% CI	(20 of 20)

CI: Confidence Interval

$$qEEG = 1 - \frac{\sum_{Interval_j} var_{Rapid}}{var_{Slow}}$$

Where:

$$var_{Rapid} \equiv \sum_{x_i \in Interval_j} \left(x_i - \overline{x_j}\right)^2$$

is the measure of rapid variance, and the measure of slow variance is the total variability:

$$var_{Slow} \equiv \sum_{i=1}^N \left(x_i - \overline{x}\right)^2$$

This qEEG measure computes a ratio of the “rapid variance” to the “slow variance.” The qEEG measure is not an f-statistic because the values in the numerator and denominator are not statistically independent of each other. Here, *qEEG* denotes the qEEG measure on the EEG voltage amplitudes *x<sub>j</sub>*, recorded at each millisecond. *Interval<sub>j</sub>* is the *j<sub>th</sub>* rapid change interval. *N* is the total number of data points in the data set. *x̄* is the mean of the voltage amplitudes of the entire data set and *x̄<sub>j</sub>* is the mean of the voltage amplitudes for the *j<sub>th</sub>* rapid change interval. Thus, we computed the sum of squared deviations for each rapid change interval, added them up, and divided this value by the sum of squared deviations for the entire data set; the measure of slow change. Finally, we subtracted this amount from one.

Compute the Ratio of DLPFC qEEG to Posterior Parietal qEEG

We compared the values of *qEEG* for the anterior EEG data to the posterior EEG data by computing the ratio:

$$qEEG\_Ratio = \frac{qEEG_{DLPFC}}{qEEG_{PosteriorParietal}}$$

Here, *qEEG\_Ratio* is the ratio, *qEEG<sub>PosteriorParietal</sub>* is the measure for the posterior parietal electrodes and *qEEG<sub>DLPFC</sub>* is the measure for the DLPFC electrodes. This ratio was computed twice; once for the delayed recognition faces task, and once for the delayed recognition objects task. These two ratios were used to compute an average ratio. *The ratio of the DLPFC qEEG measure from 151-300 ms to the posterior parietal qEEG measure for 0-150 ms will be referred to as the “qEEG ratio.”*

RESULTS  
Delayed Recognition Memory Results

Subjects’ qEEG ratios for the delayed recognition task ranged from a lowest value of 0.71 to a highest value of 1.54. These qEEG ratios had a high negative correlation with FAST scores; *ρ*= -0.71 ±0.02, 95% confidence interval, *p* < 0.001 (*t-test* based on the Fisher transform). At this alpha level (*p* < 0.001), the power of this statistical test is 99%.

qEEG ratios for 30 of the 32 normal aging subjects were greater than 1.00 (at 2 decimal places of accuracy). qEEG ratios for 14 of the 16 ADRD subjects were less than or equal to 1.00 (at 2 decimal places of accuracy). A qEEG ratio value of 1.00 yielded an optimal criterion for differentiating between ADRD and normal aging.

For the subgroup matched for age, gender and treatment, all normal aging subjects had qEEG ratios above 1.00 and all ADRD subjects had qEEG ratios less than 1.00. Using a criterion of 1.00 to differentiate between the two groups yielded the following sensitivity, specificity and total accuracy tabulated in Table 1.

Structure From Motion Results

Subjects’ qEEG ratios for the SFM task ranged from a lowest value of 0.53 to a highest value of 1.30. These qEEG ratios had a non-significant correlation with FAST scores; *ρ*= -0.06 ±0.05, 95% confidence interval. A qEEG ratio value of 0.91 yielded an optimal criterion for differentiating between ADRD and normal aging for SFM values for both the total group and the matched sample group. Using an optimal criterion of 0.91 to differentiate between the two



**Table 2**

ADRD detection: structure from motion

ADRD FAST Stages 3-4		Normal Aging		Total Accuracy
Sensitivity	Average qEEG Ratio	Specificity	Average qEEG Ratio	Overall
Total Group				
63%	0.86 ± 0.08	56%	0.90 ± 0.06	58%
(10 of 16)	95% CI	(18 of 32)	95% CI	(28 of 48)
Matched Sample Group				
80%	0.86 ± 0.09	70%	0.92 ± 0.12	75%
(8 of 10)	95% CI	(7 of 10)	95% CI	(15 of 20)

CI: Confidence Interval

groups yielded the following sensitivity, specificity and total accuracy tabulated in Table 2.

### **Delayed Recognition Memory vs. Structure From Motion**

qEEG ratios derived from delayed recognition EEG data correctly distinguished ADRD from normal aging 92% of the time. On the other hand, SFM task data distinguished ADRD from normal aging 58% of the time. A null hypothesis would be that there is no difference in accuracy between the delayed recognition memory tasks and the SFM tasks. The probability of this hypothesis being true is  $p < 10^{-6}$  (binomial test). A power analysis of this result can be made by fixing the power level to 80%. Using the formula of Hanley and McNeil,<sup>63</sup> the significance of this result is  $p < 10^{-4}$  for  $N=48$ . Similarly, the accuracy of the data for the matched sample group was 100% for the delayed recognition memory tasks and 75% for the SFM task. In this case, the probability that the null hypothesis is true is  $p < 0.005$  (binomial test). A power analysis of this result yielded a significance of  $p < 0.03$  at a power level of 80% for  $N=20$ .

### **Relative Theta Power Results**

To compare our method to a standard method, we computed the relative theta power of the subjects. The optimal sensitivity of the theta power was 75% (12 of 16) and the optimal specificity of the theta power was 75% (24 of 32). Together, these yielded a total accuracy of 75% (36 of 48). Use of the relative theta power for the gender, age and treatment matched group yielded a sensitivity of 70% (7 of 10), a specificity of 70% (7 of 10), and a total accuracy of 70% (14 of 20).

These levels of sensitivity and specificity are comparable to results in the literature.<sup>64,65</sup> We used these accuracy levels to make a statistical comparison with our delayed recognition ADRD detection method. A null hypothesis would be that our detection accuracy is no better than the theta power detection accuracy, 75% for the entire group, 70% for the age, gender and treatment matched group. The probability of the null hypothesis being true is  $p <$

0.005 (binomial test) for the entire group and  $p < 0.001$  for the age, gender and treatment matched group. A power analysis was performed on these data by fixing the power to 80% and testing for significance. This resulted in a significance of  $p < 0.05$  for the whole group,  $N=48$ , and a significance of  $p < 0.03$  for the matched sample group,  $N=20$ .

### **Correlation of Delayed Recognition**

#### **Memory and SFM qEEG Ratios**

We have hypothesized that our qEEG method yields qEEG ratios that are dependent upon the psychophysical task being performed by the subject. This implies that similar psychophysical tasks will yield similar qEEG ratios, whereas dissimilar tasks will yield different ratios. We tested this hypothesis by computing three different correlations of qEEG ratios: *Recall Faces vs. Recall Objects*, *Recall Faces vs. SFM* and *Recall Objects vs. SFM*. The results of these computations are tabulated in Table 3.

The probability that the *Recall Faces vs. Recall Objects* correlation is not different from the *SFM vs. Recall Faces* correlation is  $p < 0.005$  (z-test based on the Fisher transform). With a fixed power of 80%, this difference in correlations is significant at  $p < 0.02$ ,  $N=48$ . Similarly, the probability that the *Recall Faces vs. Recall Objects* correlation is not different from the *SFM vs. Recall Objects* correlation is  $p < 0.005$  (z-test based on the Fisher transform). This difference in correlations is significant at  $p < 0.03$  for a power level of 80%,  $N=48$ . The difference between the *SFM vs. Recall Faces* correlation and the *SFM vs. Recall Objects* correlation is not statistically significant.

### **DISCUSSION**

qEEG ratios for delayed recognition memory tasks correctly detected 14 of 16 ADRD subjects. There were 2 subjects not detected, i.e., a Type II or false negative error. We expect to see false negative subjects; however, the 2 false negative subjects may actually be the result of a treatment effect. Both subjects had recently begun cholinesterase inhibitor treatment. Both had made the subjective report that their memory had improved. Their CERAD memory test scores were normal. Our research shows that successful

Table 3		
Psychophysical task qEEG ratio correlations		
Tasks	Correlation	95%
		Confidence Interval
Recall Faces vs. Recall Objects	0.67	[0.64, 0.69]
SFM vs. Recall Faces	0.37	[0.33, 0.41]
SFM vs. Recall Objects	0.38	[0.34, 0.42]

cholinesterase inhibitor treatment can increase qEEG ratios. Thus, the results are conservative, since successful cholinesterase inhibitor treatment appears to be a confound in this qEEG study. When this potential confound was controlled for, the sensitivity of our qEEG method increased.

The qEEG ratios for the delayed recognition memory tasks also correctly classified 30 of 32 normal aging subjects. ADRD screening methods inevitably have false positives. However, it is interesting to note that the 2 false positive subjects (Type I error) were relatively young. One was in the mid 40s; the other was in the earlier 50s. Both subjects had parents with Alzheimer's Disease. Additionally, both had objective cognitive deficits. The deficit of 1 subject was left frontal cognitive impairment (verbal fluency); the other was dorsolateral-prefrontal cortical (DLPFC) cognitive impairment (working memory).

On the other hand, the qEEG ratios for the SFM task classified normal aging vs. ADRD at a chance level, 58%. The SFM task showed better classification accuracy for the age, gender and treatment matched group, 75%. However, this value was significantly less than the classification accuracy of the delayed recognition memory tasks and is only on par with traditional EEG detection methods, e.g., the relative theta power.<sup>64,65</sup> This suggests that our qEEG method is specific to the psychophysical task being performed by the subject.

More evidence for the task specific nature of our qEEG method is given by the analysis of correlations between qEEG ratios taken from different psychophysical tasks. The correlation of similar tasks, Recall Faces and Recall Objects was moderately high at 67%. On the other hand, the correlations of dissimilar tasks, Recall Faces vs. SFM and Recall Objects vs. SFM, were moderately low at 37% and 38%, respectively. Moreover, the difference between the correlation of similar tasks and the correlation of dissimilar tasks was highly significant ( $p < 0.005$ ). Again, this is evidence that our qEEG method is specific to the psychophysical task being performed by the subject.

Additional evidence for the validity of the hypothesis that our qEEG method is specific to the psychophysical task being performed by the subject comes from correlating subjects' FAST scores with qEEG ratios derived from delayed recognition memory tasks as well as from the SFM tasks. The former correlation was high at (-) 71% whereas

the latter was nearly zero at (-) 6%. Since delayed recognition memory loss is one of the first signs of dementia, the high correlation of 71% is not surprising. On the other hand, the ability to perceive structure from motion is a fairly low-level cognitive ability (MT cortex), which ought to remain intact during early ADRD. This again shows that the qEEG method is specific to the psychophysical task being performed by the subject.

The qEEG measure itself computes a value that shows how much an EEG deviates from being purely random as well as from being a constant or fixed sinusoidal signal (in all three cases, its value tends to zero). This value reflects the synchrony of the local neuronal activity, but only to the extent that the synchrony is neither absolute, nor random. That synchrony may correspond to information.<sup>1,3</sup> More specifically, the qEEG measure appears to be a statistical estimator for the Tsallis information<sup>66</sup> (Sneddon, in preparation).

Other ADRD Detection Methods

A traditional method of detecting ADRD is computing the ratio of the alpha power to the theta power. Low values indicate AD, high values indicate normal aging. Typical detection accuracies of this method are on the order of 75% for moderate AD.<sup>36</sup> They tend to be higher for severe AD and lower for mild AD.<sup>64,65</sup> Our theta power results agree with these findings.

Delays in the P300 latency also produce significant predictive power for the detection of AD.<sup>43</sup> A matched sample analysis based on the age-corrected P300 latency of 24 early ADRD and 17 normal aging subjects produced a sensitivity of 75%, a specificity of 81% and a total accuracy of 77%.

Many approaches combine multiple methods or use multiple stages of analysis for the detection of AD. For example, Duffy et al<sup>67</sup> first found the optimal brain/scalp regions and then combined the beta and theta power for AD detection. Their split-half replication study found that the beta and theta power of the posterior temporal and parietal regions appear to be the most indicative of AD. They applied this method to one half of 60 mild to moderate AD and 129 normal aging subjects in order to find the best detection criteria. Using these criteria, they detected AD vs. normal aging correctly 86% of the time on the second half of their subject group.

Another example is Jelic et al<sup>68</sup> who detected ADRD with a combination of coherence analysis and the relative theta power. They looked for the best discriminant variable to distinguish between 18 mild to moderate AD subjects and 16 healthy controls and found that the most accurate discriminant variable was a combination of the relative theta power and temporoparietal coherence. This combination produced a sensitivity of 77.8% and a specificity of 100%. Similarly, Rodriguez et al<sup>69</sup> used a combination of qEEG and measurement of regional cerebral blood flow to detect ADRD. They studied 42 MCI to moderately severe AD sub-

jects and 18 normal aging subjects. A maximum discriminant analysis produced a sensitivity of 88% and a specificity of 89%; all 5 undetected subjects had MCI to mild AD.

Other methods use variants of neural networks. These neural networks are first trained on normal and AD subjects and then applied to a new group. Petrosian et al.<sup>70</sup> combined recurrent neural networks with wavelet processing to detect mild AD. They trained their network on 3 AD and 3 normal aging subjects. The trained network was applied to 7 AD and 10 normal aging subjects. Their best training and testing results produced a sensitivity of 71%, a specificity of 100% and a total accuracy of 88%. Similarly, Benvenuto et al.<sup>71</sup> used an extended iterative projection pursuit method (two stages of projection pursuit) to detect and distinguish 15 MCI to moderately severe AD subjects from 17 control subjects. Their method yielded a sensitivity of 75%, a specificity of 100% and a total accuracy of 88%.

In general, these methods were applied to groups of mild to moderate AD subjects; CDR stages 1 and 2. Methods that used one stage of analysis had an accuracy of about 75%. Techniques that combined multiple methods or used multiple stages of analysis had accuracies of about 88%. AD detection methods that combined multiple methods or stages will generally have more free parameters than single stage methods. This means that they may be less robust.

Our detection method is a one stage process. The specifics of the method are based on the neurophysiology of delayed recognition. This method was applied to 32 normal aging and 16 very mild to mild ADRD subjects, CDR stages 0.5 and 1. Nine of the ADRD subjects scored as normals on CERAD memory tests. This method resulted in an accuracy of 92% for the total subject group. A matched

sample analysis of 20 subjects produced a sensitivity, specificity and total accuracy of 100%. One third of the ADRD subjects in the matched sample group scored as normals on CERAD memory tests.

These results should be interpreted within the context that the number of subjects in this study was small (N=48), especially in the matched sample group (N=20). This means that this study needs to be replicated with a much larger number of subjects. For this reason, the results of this study ought to be viewed as preliminary. Thus, to evaluate the robustness of this qEEG technique, larger samples are required. One clue that the discriminant criterion identified with this qEEG method may be robust is that it optimally separates normal aging from ADRD individuals at an intuitive cutoff ratio (if qEEG ratio > 1.00 ± 0.02, then normal function).

This initial estimate of the discriminant criterion will probably change with a larger population sample. However, if it remains greater than or equal to one, then it implies that a brain with a healthy delayed recognition memory yields a greater qEEG value from the dorsolateral prefrontal cortex at 151-300 ms after stimulus onset, than from the posterior parietal cortex at 0-150 ms after stimulus onset. To the extent that these electrophysiological parameters are surrogates of neurophysiological information related to the processing of delayed visual recognition, our qEEG method for the detection of ADRD should generalize to the majority of the populace.

## ACKNOWLEDGMENT

We would like to thank R. Duncan Luce and Michael Vanier for their help with this manuscript.

## REFERENCES

1. Stern EA, Bacskai BJ, Hickey GA, et al. Cortical synaptic integration in vivo is disrupted by amyloid-beta plaques. *J Neurosci* 2004; 24: 4535-4540.
2. Harris KD, Csicsvari J, Hirase H, et al. Organization of cell assemblies in the hippocampus. *Nature* 2003; 424: 552-556.
3. John ER. The neurophysics of consciousness. *Brain Res Rev* 2002; 39: 1-28.
4. Pasquier F, Grymonprez L, Lebert F, Van der Linden M. Memory impairment differs in frontotemporal dementia and Alzheimer's disease. *Neurocase* 2001; 7: 161-171.
5. Souliez L, Pasquier F, Lebert F, et al. Generation effect in short-term verbal and visuospatial memory: comparisons between dementia of Alzheimer type and dementia of frontal lobe type. *Cortex* 1996; 32: 347-356.
6. Kopelman MD. Non-verbal, short-term forgetting in the alcoholic Korsakoff syndrome and Alzheimer-type dementia. *Neuropsychologia* 1991; 29: 737-747.
7. Morris RG, Baddeley AD. Primary and working memory functioning in Alzheimer-type dementia. *J Clin Exp Neuropsychol* 1988; 10: 279-296.
8. Braak H, Del Tredici K, Bohl J, et al. Pathological changes in the parahippocampal region in select non-Alzheimer's dementias. *Ann N Y Acad Sci* 2000; 911: 221-239.
9. Smith GS, de Leon MJ, George AE, et al. Topography of cross-sectional and longitudinal glucose metabolic deficits in Alzheimer's disease: pathophysiologic implications. *Arch Neurol* 1992; 49: 1142-1150.
10. de Leon MJ, Convit A, Wolf OT, et al. Prediction of cognitive decline in normal elderly subjects with 2-[(18)F]fluoro-2-deoxy-D-glucose/positron-emission tomography (FDG/PET). *Proc Natl Acad Sci USA* 2001; 98: 10966-10971.
11. Squire LR. Memory from A to Z. *Nature* 2003; 423: 119-119.
12. Elbert T, Schauer M. Burnt into memory. *Nature* 2002; 419: 883-883.



13. Poldrack RA, Clark J, Pare-Blagoev EJ, et al. Interactive memory systems in the human brain. *Nature* 2001; 414: 546-550.
14. Squire LR. The seven sins of memory: how the mind forgets and remembers. *Nature* 2001; 413: 571-572.
15. Debanne D, Guerineau NC, Gahwiler BH, Thompson SM. Action-potential propagation gated by an axonal I-A-like K<sup>+</sup> conductance in hippocampus. *Nature* 1997; 389: 286-289.
16. Squire LR. Searching for memory: the brain, the mind, and the past - Schacter, DL. *Nature* 1996; 382: 503-504.
17. Durand GM, Kovalchuk Y, Konnerth A. Long-term potentiation and functional synapse induction in developing hippocampus. *Nature* 1996; 381: 71-75.
18. Stevens CF. Strengths and weaknesses in memory. *Nature* 1996; 381: 471-472.
19. Bunsey M, Eichenbaum H. Conservation of hippocampal memory function in rats and humans. *Nature* 1996; 379: 255-257.
20. Niedermeyer E. Frontal lobe functions and dysfunctions. *Clin Electroencephalogr* 1998; 29: 79-90.
21. Niedermeyer E. Electrophysiology of the frontal lobe. *Clin Electroencephalogr* 2003; 34: 5-12.
22. Ardekani BA, Choi SJ, Hossein-Zadeh GA, et al. Functional magnetic resonance imaging of brain activity in the visual oddball task. *Brain Res Cogn Brain Res* 2002; 14: 347-356.
23. Clark CR, Egan GF, McFarlane AC, et al. Updating working memory for words: a PET activation study. *Hum Brain Mapp* 2000; 9: 42-54.
24. Tomberg C. Cognitive N140 electrogenesis and concomitant 40 Hz synchronization in mid-dorsolateral prefrontal cortex (area 46) identified in non-averaged human brain potentials. *Neurosci Lett* 1999; 266: 141-144.
25. Johnson JS, Olshausen BA. Timecourse of neural signatures of object recognition. *J Vis* 2003; 3: 499-512.
26. Watanabe S, Kakigi R, Koyama S, Kirino E. Human face perception traced by magneto- and electro-encephalography. *Cognitive Brain Res* 1999; 8: 125-142.
27. Tomberg C, Desmedt JE. Non-averaged human brain potentials in somatic attention: the short-latency cognition-related P40 component. *J Physiol* 1996; 496 (Pt 2): 559-574.
28. Rossion B, Joyce CA, Cottrell GW, Tarr MJ. Early lateralization and orientation tuning for face, word, and object processing in the visual cortex. *Neuroimage* 2003; 20: 1609-1624.
29. Halgren E, Baudena P, Heit G, et al. Spatio-temporal stages in face and word processing. II. Depth-recorded potentials in the human frontal and Rolandic cortices. *J Physiol Paris* 1994; 88: 51-80.
30. Guillaume F, Tiberghien G. An event-related potential study of contextual modifications in a face recognition task. *NeuroReport* 2001; 12: 1209-1216.
31. Noldy NE, Stelmack RM, Campbell KB. Event-related potentials and recognition memory for pictures and words: the effects of intentional and incidental learning. *Psychophysiology* 1990; 27: 417-428.
32. Kayser J, Bruder GE, Friedman D, et al. Brain event-related potentials (ERPs) in schizophrenia during a word recognition memory task. *Int J Psychophysiol* 1999; 34: 249-265.
33. Wagner AD, Desmond JE, Glover GH, Gabrieli JD. Prefrontal cortex and recognition memory: functional-MRI evidence for context-dependent retrieval processes. *Brain* 1998; 121 (Pt 10): 1985-2002.
34. Ranganath C. The 3-D prefrontal cortex: hemispheric asymmetries in prefrontal activity and their relation to memory retrieval processes. *J Cogn Neurosci* 2004; 16: 903-907.
35. Ranganath C, Paller KA. Frontal brain potentials during recognition are modulated by requirements to retrieve perceptual detail. *Neuron* 1999; 22: 605-613.
36. Knott V, Mohr E, Mahoney C, Ilivitsky V. Quantitative electroencephalography in Alzheimer's disease: comparison with a control group, population norms and mental status. *J Psychiatr Neurosci* 2001; 26: 106-116.
37. Prichep LS, John ER, Ferris SH, et al. Quantitative EEG correlates of cognitive deterioration in the elderly. *Neurobiol Aging* 1994; 15: 85-90.
38. Dierks T, Perisic I, Frolich L, et al. Topography of the quantitative electroencephalogram in dementia of the Alzheimer type: relation to severity of dementia. *Psychiatry Res* 1991; 40: 181-194.
39. Duffy FH, Albert MS, McAnulty G. Brain electrical activity in patients with presenile and senile dementia of the Alzheimer type. *Ann Neurol* 1984; 16: 439-448.
40. Cook IA, Leuchter AF. Synaptic dysfunction in Alzheimer's disease: clinical assessment using quantitative EEG. *Behav Brain Res* 1996; 78: 15-23.
41. Knott V, Mohr E, Hache N, et al. EEG and the passive P300 in dementia of the Alzheimer type. *Clin Electroencephalogr* 1999; 30: 64-72.
42. Knott V, Millar A, Dulude L, et al. Event-related potentials in young and elderly adults during a visual spatial working memory task. *Clin EEG Neurosci* 2004; 35: 185-192.
43. Braverman ER, Blum K. P300 (latency) event-related potential: an accurate predictor of memory impairment. *Clin Electroencephalogr* 2003; 34: 124-139.
44. Pijnenburg YA, v d Made Y, van Cappellen van Walsum AM, et al. EEG synchronization likelihood in mild cognitive impairment and Alzheimer's disease during a working memory task. *Clin Neurophysiol* 2004; 115: 1332-1339.
45. Hogan MJ, Swanwick GR, Kaiser J, et al. Memory-related EEG power and coherence reductions in mild Alzheimer's disease. *Int J Psychophysiol* 2003; 49: 147-163.
46. Rugg MD, Pearl S, Walker P, et al. Word repetition effects on event-related potentials in healthy young and old subjects, and in patients with Alzheimer-type dementia. *Neuropsychologia* 1994; 32: 381-398.
47. Grunewald A, Bradley DC, Andersen RA. Neural correlates of structure-from-motion perception in macaque V1 and MT. *J Neurosci* 2002; 22: 6195-6207.
48. Bradley DC, Chang GC, Andersen RA. Encoding of three-dimensional structure-from-motion by primate area MT neurons. *Nature* 1998; 392: 714-717.
49. Lappe M. Functional consequences of an integration of motion and stereopsis in area MT of monkey extrastriate visual cortex. *Neural Comput* 1996; 8: 1449-1461.
50. Shay KA, Duke LW, Conboy T, et al. The clinical validity of the Mattis Dementia Rating Scale in staging Alzheimer's dementia. *J Geriatr Psychiatry Neurol* 1991; 4: 18-25.
51. Sclan SG, Reisberg B. Functional assessment staging (FAST) in Alzheimer's disease: reliability, validity, and ordinality. *Int Psychogeriatr* 1992; (suppl 4) 1: 55-69.

52. Reisberg B. Functional assessment staging (FAST). *Psychopharmacol Bull* 1988; 24: 653-659.
53. Jobst KA, Barnetson LP, Shepstone BJ. Accurate prediction of histologically confirmed Alzheimer's disease and the differential diagnosis of dementia: the use of NINCDS-ADRDA and DSM-III-R criteria, SPECT, X-ray CT, and Apo E4 in medial temporal lobe dementias. *Oxford Project to Investigate Memory and Aging. Int Psychogeriatr* 1998; 10: 271-302.
54. Welsh KA, Hoffman JM, Earl NL, Hanson MW. Neural correlates of dementia: regional brain metabolism (FDG-PET) and the CERAD neuropsychological battery. *Arch Clin Neuropsychol* 1994; 9: 395-409.
55. Reeves RR, Struve FA, Patrick G, et al. The effects of donepezil on the P300 auditory and visual cognitive evoked potentials of patients with Alzheimer's disease. *Am J Geriatr Psychiatry* 1999; 7: 349-352.
56. Knott V, Mohr E, Mahoney C, Ilivitsky V. Pharmacologic test dose response predicts cholinesterase inhibitor treatment outcome in Alzheimer's disease. *Methods Find Exp Clin Pharmacol* 2000; 22: 115-122.
57. Hermens DF, Williams LM, Lazzaro J, et al. Sex differences in adult ADHD: a double dissociation in brain activity and autonomic arousal. *Biol Psychol* 2004; 66: 221-233.
58. Widagdo MM, Pierson JM, Helme RD. Age-related changes in qEEG during cognitive tasks. *Int J Neurosci* 1998; 95: 63-75.
59. Duffy FH, McAnulty GB, Albert MS. The pattern of age-related differences in electrophysiological activity of healthy males and females. *Neurobiol Aging* 1993; 14: 73-84.
60. Johannsen P. Long-term cholinesterase inhibitor treatment of Alzheimer's disease. *CNS Drugs* 2004; 18: 757-768.
61. Williams BR, Nazarians A, Gill MA. A review of rivastigmine: a reversible cholinesterase inhibitor. *Clin Ther* 2003; 25: 1634-1653.
62. Niedermeyer E, Lopes da Silva FH. *Electroencephalography: basic principles, clinical applications, and related fields*. 4th ed. Baltimore, MD: Williams & Wilkins; 1999: 1258.
63. Hanley J, McNeil B. A method of comparing the areas under receiver operating characteristic curves derived from the same cases. *Radiology* 1983; 148: 839-843.
64. Belouchrani A. Discrimination of Alzheimer's disease and normal aging by EEG data. *Electroencephalogr Clin Neurophysiol* 1997; 103: 241-248.
65. Anderer P, Saletu B, Kloppe B, et al. Discrimination between demented patients and normals based on topographic EEG slow wave activity: comparison between z statistics, discriminant analysis and artificial neural network classifiers. *Electroencephalogr Clin Neurophysiol* 1994; 91: 108-117.
66. Tsallis T C. Possible generalization of Boltzmann-Gibbs statistics. *J Statistic Physics* 1988; 52: 479-487.
67. Duffy FH, McAnulty GB, Albert MS. Temporoparietal electrophysiological differences characterize patients with Alzheimer's disease: a split-half replication study. *Cereb Cortex* 1995; 5: 215-221.
68. Jelic V, Wahlund LO, Almkvist O, et al. Diagnostic accuracies of quantitative EEG and PET in mild Alzheimer's disease. *Alzheimers Rep* 1999; 2: 291-298.
69. Rodriguez G, Nobili F, Rocca G, et al. Quantitative electroencephalography and regional cerebral blood flow: discriminant analysis between Alzheimer's patients and healthy controls. *Dement Geriatr Cogn Disord* 1998; 9: 274-283.
70. Petrosian AA, Prokhorov DV, Lajara-Nanson W, Schiffer RB. Recurrent neural network-based approach for early recognition of Alzheimer's disease in EEG. *Clin Neurophysiol* 2001; 112: 1378-1387.
71. Benvenuto J, Jin Y, Casale M, et al. Identification of diagnostic evoked response potential segments in Alzheimer's disease. *Exp Neurol* 2002; 176: 269-276.